Climate Dynamics
https://doi.org/10.1007/s00382-024-07165-7

ORIGINAL ARTICLE

# Describing future UK winter precipitation in terms of changes in local circulation patterns

David M. H. Sexton[1] · Carol F. McSweeney[1] · Philip E. Bett[1] · Fai Fung[1] · Hazel E. Thornton[1] · Kuniko Yamazaki[1]

Received: 26 October 2023 / Accepted: 14 February 2024


**Abstract**
Social scientists have argued that good communication around risks in climate hazards requires information to be presented in a user-relevant way, allowing people to better understand the factors controlling those risks. We present a potentially useful way of doing this by explaining future UK winter precipitation in terms of changes in the frequency, and associated average rainfall, of local pressure patterns that people are familiar with through their use in daily weather forecasts. We apply this approach to a perturbed parameter ensemble (PPE) of coupled HadGEM3-GC3.05 simulations of the RCP8.5 emissions scenario, which formed part of the UK Climate Projections in 2018. The enhanced winter precipitation by 2050–99 is largely due to an increased tendency towards westerly and south-westerly conditions at the expense of northerly/easterly conditions. Daily precipitation is generally more intense, most notably for the south-westerlies. In turn, we show that the changes in the frequency of the pressure patterns are consistent with changes in larger scale drivers of winter circulation and our understanding of how they relate to each other; this should build user confidence in the projections. Across the PPE, these changes in pressure patterns are largely driven by changes in the strength of the stratospheric polar vortex; for most members the vortex strengthens over the twenty-first century, some beyond the CMIP6 range. The PPE only explores a fraction of the CMIP6 range of tropical amplification, another key driver. These two factors explain why the PPE is skewed towards exploring the more westerly side of the CMIP6 range, so that the PPE's description of UK winter precipitation changes does not provide a full picture.

**Keywords** Ensemble climate projections · Perturbed parameter ensembles · Weather types · UK climate projections

## 1 Introduction

One of the key aspects of making good decisions about how to adapt to climate change is that there is effective communication between specialists and users, particularly around the handling of the uncertainty inherent in the projections (Jones et al. 2015). Pidgeon and Fischhoff (2011) argue that for good communication around climate risks, people also need some understanding of "the processes creating and controlling those risks, and thus causing uncertainty about them". In this spirit, and as providers of the UK Climate Projections 2018 (UKCP18; Murphy et al. 2018), our main goal here is to provide a physical explanation of the range of changes in UK winter precipitation which (a) users can easily relate to, and (b) allows them to assess the robustness of the projections. We focus on the 15-member perturbed parameter ensemble (PPE) of HadGEM3-GC3.05 simulations (Yamazaki et al. 2021). The PPE members differ by having different values for 47 parameters in the atmosphere/land schemes covering convection, the boundary layer, gravity wave drag, cloud microphysics, cloud radiation, the land surface and aerosols. The same ocean configuration was used for each member and the simulations are flux-adjusted. These 15 PPE members were combined with 13 CMIP5 simulations to provide "UKCP Global", the plausible global realisations in UKCP18 (Murphy et al. 2018). Therefore, our results will be of immediate relevance to studies of climate biases and impacts (e.g., Arnell et al. 2020; Hanlon et al. 2021; Kennedy-Asser et al. 2021; Garry and Bernie 2023) already based on UKCP Global and "UKCP Regional" and "UKCP Local", the regional model simulations at 12km and

✉ David M. H. Sexton
david.sexton@metoffice.gov.uk

[1] Met Office Hadley Centre, FitzRoy Road, Exeter EX1 3PB, UK

Published online: 21 March 2024

2.2km resolution downscaled from 12 of the 15 PPE members (Fosser et al. 2020; Kendon et al. 2021).

Our approach involves two stages. First, we aim to describe the uncertainty of some aspect of the future climate in terms that people can more easily relate to. Our approach complements other new ways in which climate scientists are trying to help people understand what future climate might mean for our everyday lives (e.g. BBC 2020). In our example, we will explain the range of changes in UK winter precipitation in terms of changes in common pressure patterns over the UK ("weather types") and in their associated precipitation. Pressure patterns have the advantage that they are already familiar to members of the UK public through their use by weather presenters on British television to explain uncertainty in the forecast. The emphasis here is on providing a useful description. This is in contrast with an index like the North Atlantic Oscillation (NAO), which is the primary mode of atmospheric variability in the North Atlantic, and is useful for demonstrating skill in forecasts from a season out to one year ahead (Scaife et al. 2014a; Dunstone et al. 2016). However, the NAO is a feature best suited for describing the climate on monthly to seasonal timescales, exhibiting large variation in daily conditions for a given phase of the NAO; several of the weather types used here project on to the NAO pattern yet behave differently to each other in our climate projections. Using the NAO index here would lose useful detail in the explanation.

The second stage involves linking the changes in the pressure systems to the larger scale drivers of circulation like the stratospheric polar vortex or upper tropical tropospheric warming. Such drivers have been used to explain seasonal forecasts, and feature in explanations of recent extreme UK winters (Huntingford et al. 2014; Davies et al. 2021). They have been used to explain a large fraction of the spread of the projected changes in the CMIP5 ensemble (Manzini et al. 2014). This has led to their use as the basis for a storyline approach (Zappa and Shepherd 2017) to aid decision-making, and for that same reason, we use them in our second stage to assess how representative our PPE is of the uncertainty that could be explored by combinations of different sets of climate projections (e.g. the PPE, a multimodel ensemble, a single model ensemble with a large number of initial conditions e.g. Kay et al. (2015), or a one-off very expensive, very high resolution simulations e.g. Moreno-Chamarro et al. (2021)). Such an assessment aids robust decision-making by using deeper process understanding to provide the user with more tools for judging the usability and limitations of the information, and this step is considered a key ingredient for building confidence in model projections (Baumberger et al. 2017).

In this study, we focus on the 15-member PPE of HadGEM3-GC3.05 coupled simulations rather than the combined set of CMIP5 and PPE members used in the UKCP18 Global Projections. This is firstly because we want to demonstrate how to assess the robustness of a single source of projections like the PPE against a wider context (here the CMIP6 ensemble). This makes our results particularly relevant to studies based on UKCP Regional and UKCP Local, which are based entirely on PPE members. Multimodel ensembles like CMIP5 and CMIP6 are useful context as they typically provide a wider range of climate projections than a PPE based around a single model because they explore more processes (Collins et al. 2011). However, in practice, the situation depends on the climate variable of interest. Yamazaki et al. (2021) show that our PPE explores a reasonably diverse set of regional precipitation changes for most worldwide regions, but a narrow range of global warming relative to CMIP5. The latter demonstrates the presence of a structural limitation that is, by definition, common to all parameter combinations. In contrast, each member of the multimodel ensemble has their own systematic error, and this will not be well understood unless there is an associated PPE. Rostron et al. (2020) shows that for some variables, the bias in the tuned variant might not be a good indicator of the structural error common to most PPE members. This lack of explicit understanding of the different structural errors of the multimodel ensemble members has long been ignored in emergent constraints but it has presented issues, for example, such relationships might lack robustness across successive CMIP ensembles (Caldwell et al. 2018). Here we use emergent relationships to link the changes in UK winter precipitation to a) large-scale drivers and b) the key parameters and processes that are driving the variation in this single model framework. So, the second reason for focusing on the PPE is that these emergent relationships are based on PPE members with a single common systematic error, and can be linked to parameter perturbations, which will be indicative of a physical mechanism. In other words, emergent relationships across a PPE are more clearly interpreted, albeit in the context of this particular structural limitation.

In Sect. 2, we describe details of the 15-member PPE of HadGEM3-GC3.05 coupled simulations and the circulation variables that will be analysed. Section 3 describes changes in the frequency of pressure patterns classified into eight "weather types". In Sect. 4, changes in UK winter precipitation are decomposed into changes in the frequency of each weather type, and changes in the average rainfall associated with each weather type. This decomposition is then used to explain the range of changes in UK winter precipitation and its interannual variability across the PPE. Section 5 investigates the links to changes in the eddy-driven jet and other large-scale circulation drivers to assess the robustness of the PPE projections. Section 6 summarises the results and discusses how they might support user applications.

## 2 Experimental details and data

We analyse the 15 members of the PPE of HadGEM3-GC3.05 coupled simulations under CMIP5 historical and RCP8.5 emissions scenarios that contributed to UKCP Global. The details about the parameter perturbations and various stages of the coupled experiments can be found in Yamazaki et al. (2021). Five other PPE members were omitted from UKCP18 due to obvious drifts in their Atlantic Meridional Overturning Circulation (AMOC). Since the release of UKCP18, control simulations of 1900 conditions have been run for each of the PPE members and have revealed that two members of UKCP18 (with id numbers 2305 and 2335 following Yamazaki et al. (2021)) also have drifts in their AMOC. We retain these two members here as they are already in UKCP-based studies. The PPE members are the same resolution (60km atmosphere, quarter degree ocean) as used in the Met Office seasonal forecasts which have skill at predicting the winter NAO (Scaife et al. 2014a). The model configuration is very similar to HadGEM3-GC3.1 (Williams et al. (2018)), which is used for climate simulations provided by the Met Office to CMIP6 and has been shown to capture the frequency of various weather regimes relatively well compared to other climate models (Fabiano et al. 2020). The small differences between the GC3.05 and GC3.1 configurations are explained in Sexton et al. (2021), as is the method for picking the parameter combinations. The control simulations are used in Sect. 5.

We analyse the precipitation changes from 1900 to 2100 over five regions: the UK, Scotland, Northern Ireland, Wales, and England. We only consider grid points where the land fraction is greater than 0.5. In Sect. 4 we focus on the difference between the last fifty years of the simulation relative to the first 50 years, that is, 2050–2099 minus 1900–1949. For similar reasons to Zhang et al. (2021), this choice provides the strongest signal with a baseline period largely unaffected by anthropogenic forcing.

There are several different methods for estimating weather types. We use a method (Fereday et al. 2008; Neal et al. 2016) based on k-means clustering to classify daily mean circulation patterns for the full period 1900–2100; hereafter we refer to these clusters as "weather types" in line with terminology used in UKCP18. The Met Office routinely classifies pressure patterns over the North Atlantic and European sector into a pre-defined number of weather types, and uses them as a tool for weather forecasting and extreme event analysis (Neal et al. 2016; Kendon et al. 2020). Here we use the classification into 8 weather types which describe the broad-scale features of the atmospheric circulation. There are alternatives, e.g. the four patterns used by Madonna et al. (2017), but the eight weather types have the advantage that they are available online to users of UKCP18. The eight weather types are also based on mean sea level pressure rather than geopotential height and so are more relevant to the UK public. See Pope et al. (2021) for a description of changes in the 30 weather types in UKCP18 Global, which are a more detailed classification on which our eight are based. Note that we assume the eight weather types are relevant to the future as well as the historical climate so that error from any misclassification is small. Neal et al. (2016) name the eight weather types (see Fig. S1) as 1: NAO- (Northerly); 2: NAO + (Westerly); 3: Northwesterly; 4: Southwesterly; 5: Scandinavian High; 6: UK High; 7: UK Low (low pressure centred just to west of UK); and 8: Azores High. The names in brackets for the first two weather types are ones we use here in the paper, but we note that NAO- covers a wide range of pressure patterns ranging from Northerly to Northeasterly (see Fig. S2).

Alternative methods for classifying the atmospheric circulation exist, such as principal component analysis of the mean sea level pressure field e.g. Woollings et al. (2010). However, the resultant eigenvectors are not necessarily physical, rather a mathematical description and not as familiar to people as the pressure patterns represented by the weather types. So, weather typing is preferred here to describe atmospheric variability.

To understand the links between UK winter precipitation and the large-scale circulation we analyse relationships with the eddy-driven jet, tropical and extra-tropical temperatures, stratospheric circulation (Zappa and Shepherd 2017) and the QBO (Andrews et al. 2019). For the midlatitude jet driven by momentum and heat fluxes from transient midlatitude eddies, we use daily diagnostics that measure the jet latitude and strength based on 850hPa zonal wind speed (Woollings et al. 2010). That study identified three preferred jet latitude bands linked to the dominant patterns of atmospheric variability in the North Atlantic. These are (i) a southern jet where the wind speed peaks at a latitude similar to Spain; (ii) a central jet where the greatest speeds are just to south of the UK; and (iii) a northern jet that passes north of Scotland. As the jet stream shifts north, there is an increase in the southwest-northeast tilt. There is substantial intra-seasonal to inter-annual variability in the eddy-driven jet that determines much of the winter weather in the North Atlantic-European sector.

Daily time series of the weather types and jet diagnostics are available online as part of UKCP18 under "UKCP18 European Circulation Indices" (Met Office Hadley Centre 2020). Murphy et al. (2018) show that the PPE reproduces the tri-modal distribution of the jet latitude relatively well compared to the 13 CMIP5 models used in UKCP18. They also show that the frequency of weather types found in the PPE is also reasonable, although there

is a small systematic tendency to have too many cases of WT1 (Northerly) at the expense of WT3 (Northwesterly).

The three indices from Zappa and Shepherd (2017) that are important drivers of Northern Hemisphere extratropical circulation are: polar amplification (850hPa temperature averaged 60–90°N); tropical amplification (250hPa temperature averaged 30°S–30°N); and stratospheric polar vortex strength (20hPa westerly wind speed averaged 70–80°N; we drop "stratospheric" hereafter). We also include the QBO (20hPa westerly wind averaged 10°S–10°N) as Holton and Tan (1982) have shown that it is related to Northern Hemisphere winter circulation. Indeed, studies have shown that the QBO influences seasonal forecasts of circulation over the Atlantic (Scaife et al. 2014b; Maidens et al. 2021).

The aim is to use these large-scale drivers to assess the robustness of our climate projections by assessing to what extent the PPE explores the range sampled by other climate models. For this exercise, we use CMIP6 simulations (see Table 1; Eyring et al. 2016).

**Table 1** List of CMIP6 models used in this study. Only one variant is used for each model, and this is indicated by the Variant-Id

| Model | Institution | Variant-Id |
|---|---|---|
| ACCESS-CM2 | CSIRO-ARCCSS | r1i1p1f1 |
| ACCESS-ESM1-5 | CSIRO | r1i1p1f1 |
| AWI-CM-1–1-MR | AWI | r1i1p1f1 |
| BCC-CSM2-MR | BCC | r1i1p1f1 |
| CAMS-CSM1-0 | CAMS | r1i1p1f1 |
| CESM2 | NCAR | r1i1p1f1 |
| CESM2-WACCM | NCAR | r1i1p1f1 |
| CMCC-CM2-SR5 | CMCC | r1i1p1f1 |
| CanESM5 i1p1f1 | CCCma | r1i1p1f1 |
| FGOALS-g3 | CAS | r1i1p1f1 |
| FIO-ESM-2–0 | FIO-QLNM | r1i1p1f1 |
| GISS-E2-1-G | NASA-GISS | r1i1p1f2 |
| HadGEM3-GC31-LL | MOHC | r1i1p1f3 |
| HadGEM3-GC31-MM | MOHC | r1i1p1f3 |
| IITM-ESM | CCCR-IITM | r1i1p1f1 |
| MCM-UA-1–0 | UA | r1i1p1f2 |
| MIROC-ES2L | MIROC | r1i1p1f2 |
| MIROC6 | MIROC | r1i1p1f1 |
| MPI-ESM1-2-HR | MPI-M | r1i1p1f1 |
| MPI-ESM1-2-LR | MPI-M | r1i1p1f1 |
| MRI-ESM2-0 | MRI | r1i1p1f1 |
| NESM3 | NUIST | r1i1p1f1 |
| NorESM2-LM | NCC | r1i1p1f1 |
| NorESM2-MM | NCC | r1i1p1f1 |
| TaiESM1 | AS-RCEC | r1i1p1f1 |
| UKESM1-0-LL | MOHC | r1i1p1f2 |

## 3 Changes in local drivers of UK winter weather

Figure 1 (top panel) shows the ensemble mean change in the number of days that each weather type occurs during each winter. There is an increase in frequency for weather types 2 and 6 (Westerly and UK High) from about 2000 onwards. This increase in frequency is common to all 15 PPE members by the end of the twenty-first century (middle panel) and is associated with modest increases in year-to-year variability in frequency by the end of the twenty-first century. Southwesterlies (WT4) also increase in frequency for nearly all members and the ensemble mean suggests this starts middle of the twenty-first century. These increases in frequency are balanced by a decrease in frequency of weather types 1 and 5 (Northerly and Scandinavian High) over nearly all PPE members, both accompanied by a reduction in the year-to-year variability of their frequency during the twenty-first century. If we consider weather types 1, 2, and 5 to be similar to the regimes NAO − , NAO + and Scandinavian Blocking (SBL) of Fabiano et al. (2021), then the PPE behaves similarly to CMIP6 for NAO + and SBL, but only like half of the CMIP6 simulations that show a reduced frequency of NAO-. Fig. S3 shows that these changes are outside the range of deviations of individual members about the ensemble mean after filtering to remove annual and decadal variability. Weather types 3, 7, and 8 (Northwesterlies, UK Low, and Azores High) do not change much in terms of frequency or year-to-year variability.

## 4 Changes in projected UK winter rainfall and its variability and links to weather types

Figure 2 shows that winter mean precipitation is projected to increase in all five regions. The strongest signals are in Scotland and Wales, which show a more rapid increase from 2030 onwards. Comparison with an estimate of the observed climatological average for 1985–2014 from E-OBS (see Fig. S4; Haylock et al. 2008) shows that in the ensemble mean, the PPE has a wet bias for Wales, England, and the UK of 15%, 27%, and 15% respectively, whereas Scotland and Northern Ireland have very small biases. We assume that this bias to continue into the twenty-first century. There is a modest rise in year-to-year variability, which is most strongly seen in Wales from 2025 onwards. This increased winter precipitation and increased range of winter precipitation seen from year to year will present a major adaptation challenge. For Wales

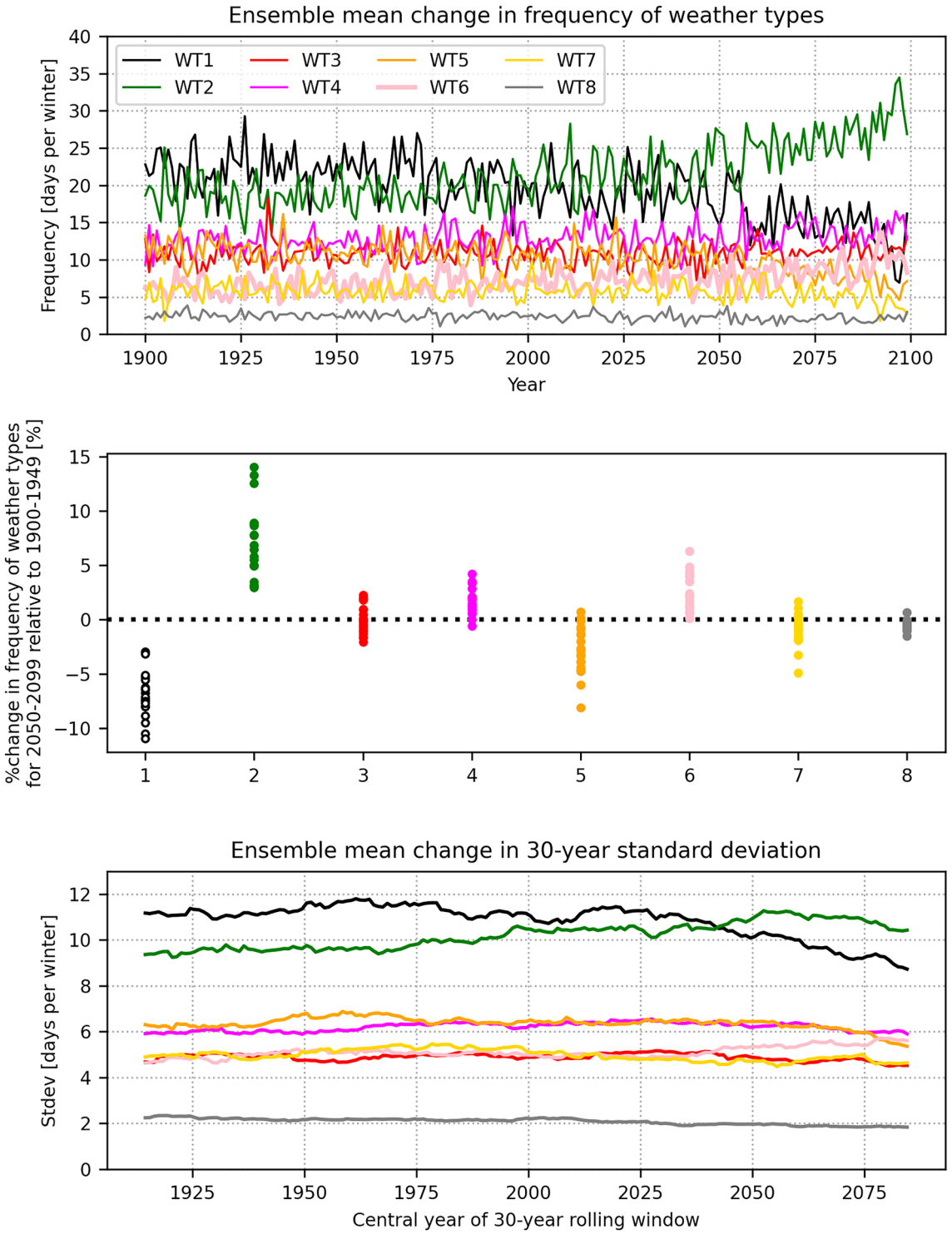


**Fig. 1** Changing frequency of weather types and their year-to-year variability for DJF in 1900–2100 (top panel) Change in frequency of each of the 8 weather types for the 15-member ensemble average; (middle panel) Change in frequency between 2050–99 and 1900–49 for each of the 8 weather types for each member; (bottom panel) Change in the ensemble mean of the interannual standard deviation of the frequency of each weather type over a rolling 30-year window plotted against the central year of the window

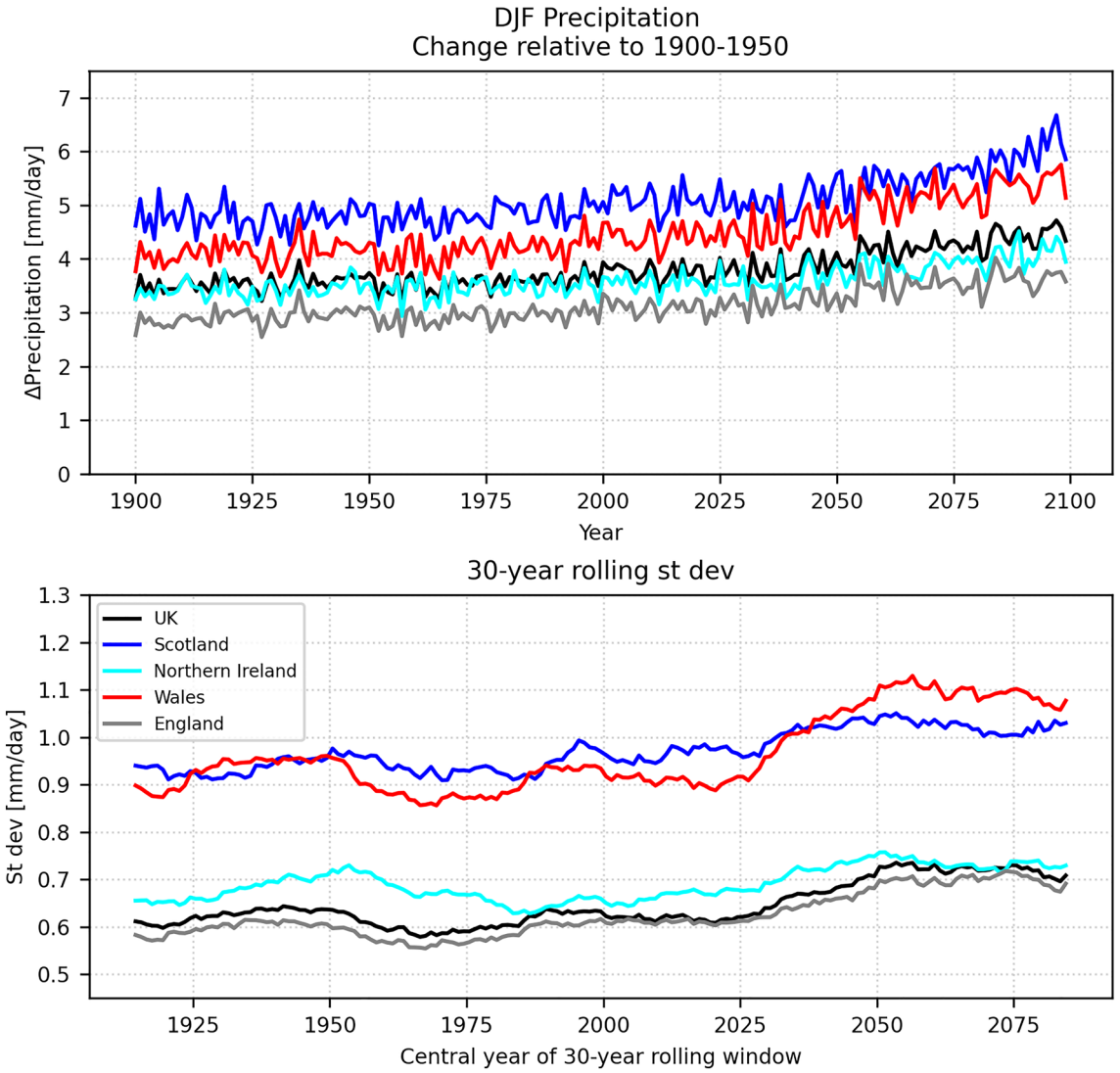


**Fig. 2** Change in winter precipitation in the five different regions. (top panel) Ensemble average of DJF mean precipitation change relative to 1900–1950; (bottom panel) Ensemble average of the interannual standard deviation of DJF mean precipitation in a rolling 30-year window

there is a heightened risk of the interannual variability doubling by the end of the twenty-first century, as a few members have a standard deviation that is about twice the ensemble average value seen in the 1900–1949 baseline (not shown). Therefore, it is important to understand what is driving the range of changes in winter precipitation and its interannual variability.

An approach that has proved useful for understanding precipitation changes, is based on the decomposition of the changes in to a dynamic/non-thermodynamic and thermodynamic/non-dynamic component. These methods vary in complexity from the detailed budget analysis of Seager et al. (2010) to the simpler method adopted by Emori and Brown (2005) where precipitation was conditioned on a dynamical variable, in their case the intervals in the strength of vertical ascent. We use the simple method here as it is versatile, having been applied successfully to other problems e.g. understanding cloud changes (Bony et al. 2004) and cloud radiation in the tropics (Williams and Webb 2009).

The difference here is that the dynamic component is conditioned on the weather types. For a given period, we categorise the days into different weather types (i = 1,…,8 here). For each weather type we estimate the average amount of precipitation per day, which we will refer to as "intensity". Then the precipitation ($p$) for that period, is the sum of the intensities ($I$) weighted by the frequency ($f$) over 8 weather types. For a given PPE member, the precipitation in the baseline period is,

$$p^{base} = \sum_{i=1}^{8} f_i^{base} I_i^{base} \quad (1)$$

The same can be applied to a future period with different frequencies and different average precipitation for each weather type. If the future values of frequency and intensity are expressed as changes from the baseline values (denoted by Δ's), then

$$p^{fut} = \sum_{i=1}^{8} f_i^{fut} I_i^{fut} = \sum_{i=1}^{8} (f_i^{base} + \Delta f_i)(I_i^{base} + \Delta I_i) \quad (2)$$

The change in precipitation can then be written as:

$$p^{fut} - p^{base} = \sum_{i=1}^{8} (\Delta f_i \bullet I_i^{base} + f_i^{base} \bullet \Delta I_i + \Delta f_i \bullet \Delta I_i) \quad (3)$$

Equation 3 shows that the change in precipitation is made up of three terms: (i) the change in frequency multiplied by the baseline intensity; (ii) the baseline frequency multiplied by the change in intensity; and (iii) a cross term multiplying the changes in frequency by the changes in intensity. We describe the first term as the "dynamic" contribution, as it is due solely due to the changes in the frequency of the weather types. The second term arises solely from the change in intensity under each weather type. Intensity is due to a number of reasons such as moisture availability, contrast between the temperature and humidity of the polar and tropical air masses, how deep the low-pressure system becomes, plus other mechanisms that affect rainfall on a few occasions like interaction with dry air from the stratosphere. The first two reasons are thermodynamic, though the third reason involves both thermodynamics and dynamics in how the air is advected across jet exit regions. Therefore, we do not label this term as "non-dynamic" or "thermodynamic". We also note that the 60km horizontal resolution used in our PPE will represent the large-scale circulation better than smaller scale processes that can drive rainfall intensity. Smaller scale features are better captured by very high resolution convection-permitting models (Fosser et al. 2020).

For a given PPE member, the change in frequency for each of the weather types, $\Delta f_i$, has been shown in Fig. 1 (middle panel). For the changes in intensity for 2050–2099 (see Fig. 3), it is clearer to present them as percentage changes from the 1900–1949 baseline value i.e., $100 \times \Delta I_i / I_i^{base}$. For weather types 4–8, most members show an increase in intensity over all five regions. Weather type 1 (Northerly) events largely become wetter in Wales (up to 50%), but largely drier in Scotland (up to 30%) with no clear sign of change for Northern Ireland and England. Westerly days (WT2) become wetter across the PPE for Wales and England but there is no robust signal for Northern Ireland or Scotland. Northwesterlies (WT3) become drier in Scotland and Northern Ireland but have no consistent change in England and Wales.

The total precipitation change can be decomposed into contributions from the 8 weather types for individual members (as an example see Fig. S5 for UK) and then averaged across the 15 ensemble members (Fig. 4). The ensemble-averaged results (top left) show that the biggest increase in winter precipitation generally involves weather types 2 and 4 (westerlies and south-westerlies), but these are partly offset by negative changes associated by weather type 1 (northerly). Weather type 6 also shows a small positive ensemble mean change. Other weather types make small contributions for some of the PPE members (Fig. S5a). The observational biases described above suggest that any bias adjustment would modify the results for England the most, then Wales and UK, but have little impact on those for Scotland and Northern Ireland.

A main aim of this paper is to explain what is driving the spread in winter precipitation changes in terms of intensity and frequency of the eight weather types. This means identification of the weather types that cause the most deviation of the individual members about their respective ensemble mean contribution. For a given weather type and quantity, this is measured as the total variance, that is the sum of the row of the covariance matrix including the off-diagonal terms associated with the other weather types. The second of the three bars in Fig. 4 (top right) shows that for all five regions, the total variance is dominated by weather type 2 (westerlies). For Scotland, there is a secondary contribution from weather type 3 (northwesterly) offset by negative contributions from weather type 5 (Scandinavian High). For other regions, the southwesterlies (WT4), which provided the second largest ensemble mean contribution, do not contribute much to the spread indicating that their contribution is consistent across the ensemble.

The cyan and grey bars in Fig. 4 (top left) show that the main contributions to total changes in UK and regional winter precipitation are associated with changes in the average daily rainfall associated with each weather type (i.e., the intensity term) rather than changes in the frequency of the weather types. Scotland is an exception in that there is a more equal split between frequency and intensity. Figure 4 (top right) shows that the intensity dominates the spread in winter precipitation changes for all five regions.

The effect of a change in intensity or a change in frequency can be decomposed into contributions from each weather type. Figure 4 (middle panels) show that the ensemble mean increase in precipitation results from most WTs seeing an increase, with the largest contribution from weather type 4 (south westerly) followed by type 2 (Westerly). For the variance in the change in the intensity, weather types 1, 2, and 4 provide the main contribution across any of the five regions. Figure 4 (bottom panels) show that the ensemble means of precipitation change associated with frequency changes, are dominated by weather type 2 (Westerly). The variance from the change in frequency is small for all regions except for a modest contribution for Scotland.

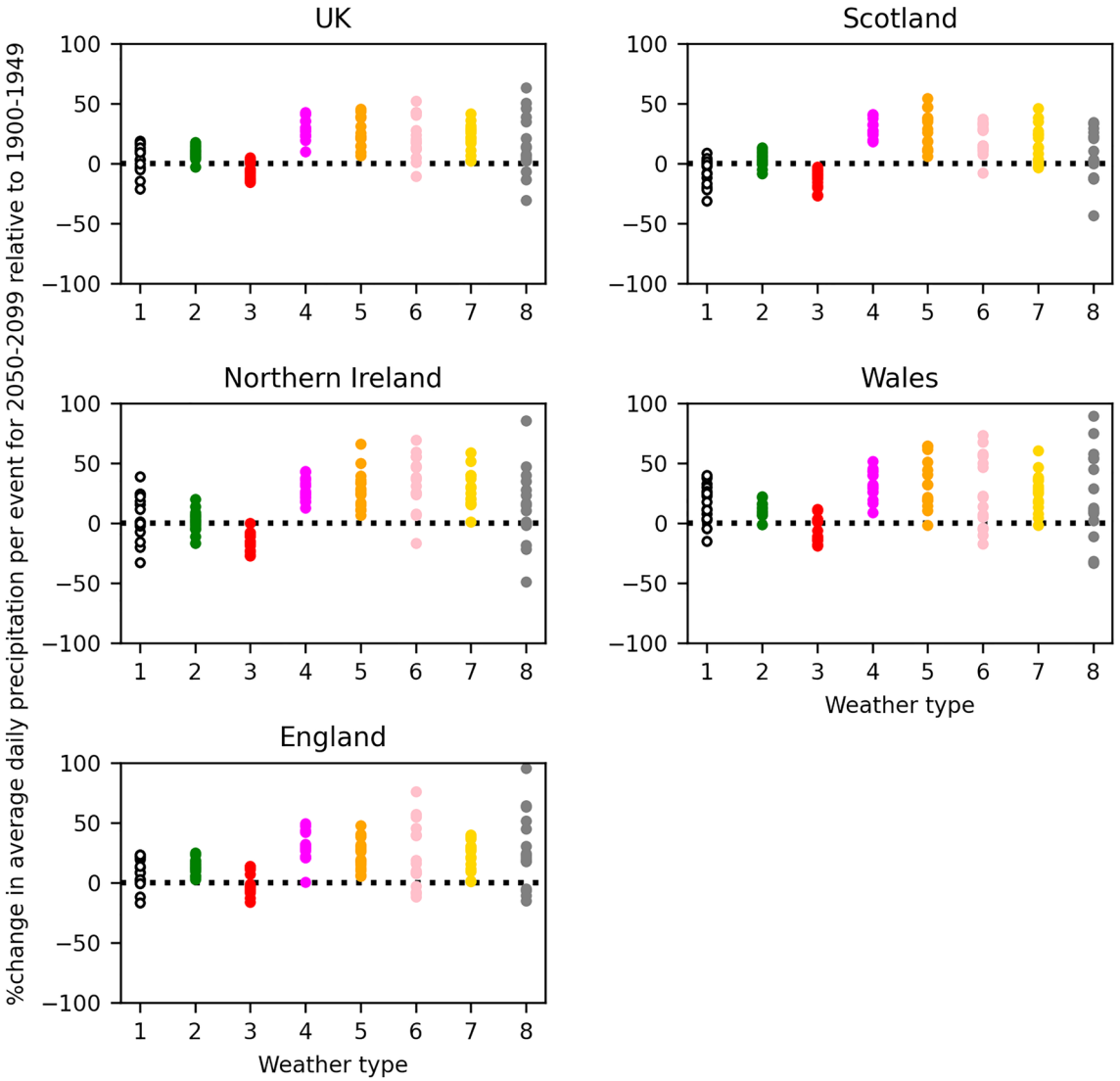


**Fig. 3** Percentage changes in intensity (average daily rainfall) from 1900–1949 to 2050–2099 for each of the 8 weather types and for each of the five regions. The colour coding for the weather types is the same as used in Fig. 1

In this case, the variance associated with westerlies is moderately large, but it is offset by a reduction in frequency of Northerlies and Scandinavian High (WT5).

In summary for the UK, the increase in winter precipitation in the future arises due to both a change in the relative frequency of individual weather types (particularly more westerlies) and an increase in the intensity of precipitation associated with most weather types. South-westerlies (WT4) consistently contribute the second largest increase in precipitation, more through changes in intensity than frequency. A reduction in frequency of northerly flow (WT1) partly offsets the two main positive contributors. The picture is largely the same for regions of the UK with Wales and Scotland having the greatest precipitation change into the future. Relative contributions from frequency and precipitation intensity changes are similar to those for the UK, with Scotland affected most by changes in frequency, Wales most by changes in intensity. The spread in changes in winter precipitation is most affected by variations in the changes associated with westerlies, more so in Scotland and Wales, and less in Northern Ireland.

An important consideration for adaptation is associated with changes in year-to-year precipitation variability as an increase over time means that society would need to adapt to a wider range of weather conditions. Figure 5 shows that on average across the PPE there is an increase in year-to-year variability of winter precipitation for all five regions over the twenty-first century. To diagnose the contribution of year-to-year changes in precipitation due to changes in frequency (yellow line), we reconstruct the precipitation

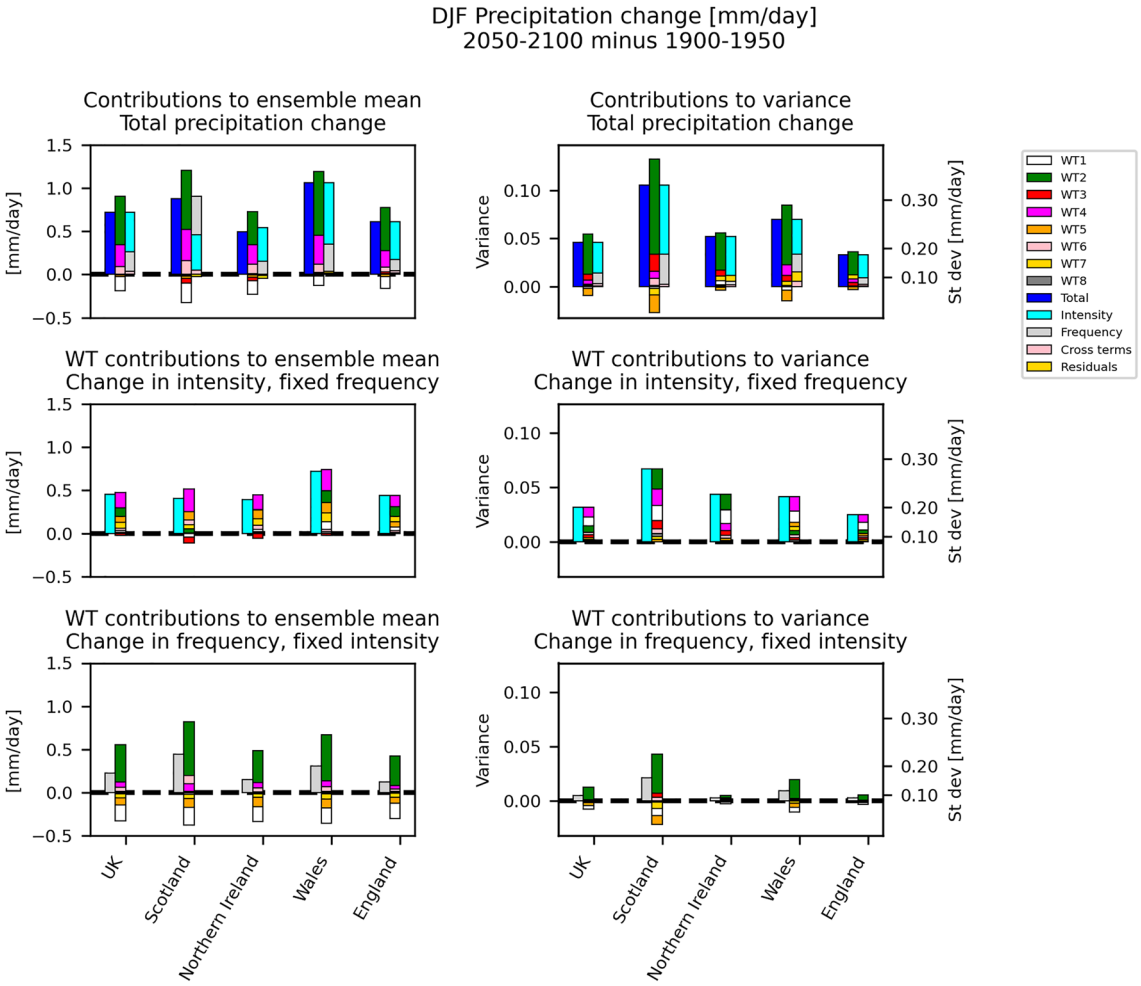


**Fig. 4** Summary over the five regions of ensemble mean (left panels) and ensemble variance (right panels) explained by different contributions of the frequency and intensity to the total winter precipitation changes from 2050–2100 relative to 1900–1950. (top panels) The values correspond to the ensemble mean and variance and show 3 bars: the total; contributions from each weather type; and contributions from the frequency, intensity and cross-terms; (middle panels) Decomposition based on weather type for the ensemble average and variance where intensity is allowed to vary with time but frequency is fixed at its baseline value; (bottom panels) Decomposition based on weather type for the ensemble average and variance, where frequency is allowed to vary with time and intensity is fixed at its baseline value

time series from the sum of the time series of frequency (see Fig. 1) for a given weather type scaled by its baseline average intensity. We then estimate the rolling window of year-to-year variability. We follow the equivalent procedure to estimate the effect from year-to-year changes in intensity (red line). In all regions over all time windows, changes in year-to-year variations in the intensity of the precipitation is the dominant contribution to precipitation variability. Changes in interannual precipitation variability from changes in frequency of weather types are steady for all regions and, apart from in Scotland, are often appreciably lower than the contribution from intensity. Consequently, the increase in winter precipitation variability is largely associated with increases in year-to-year variations in precipitation intensity.

## 5 Changes in large-scale circulation and key drivers

In this section we analyse the eddy-driven jet and other large-scale drivers of circulation to a) better explain what is driving variations in the weather types that affect the UK winter precipitation changes so that we can b) assess the robustness of the projections provided by the PPE.

### 5.1 Eddy-driven jet

First, we focus on showing that the changes in frequency of the weather types are qualitatively consistent with

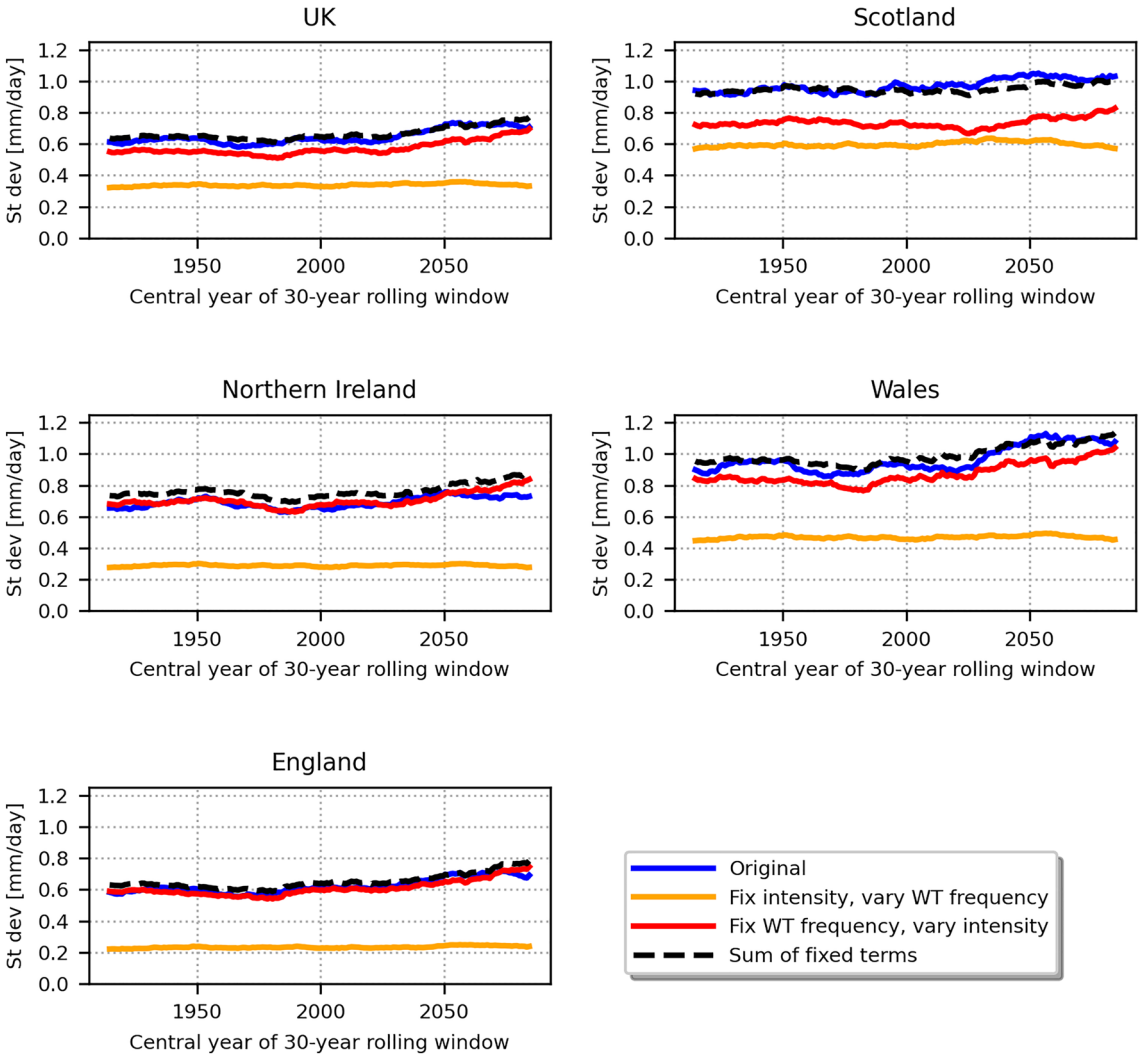


**Fig. 5** Contribution in year-to-year variability of regional precipitation associated with weather type frequency and intensity changes. The black dashed line is the ensemble mean of the standard deviation over a rolling 30-year window from time series of winter precipitation. The yellow line ('fixed intensity) is like the black line but based on time series generated by scaling the changes in weather type frequency by the 1900–1949 average intensity. Likewise, the red line is based on time series of changes in intensity scaled by their 1900–1949 average frequency. The blue line is the square root of the yellow and red lines added in quadrature

changes in the most immediate large-scale driver of flow over the North Atlantic/Europe sector, the eddy-driven jet. The observed relationship has been demonstrated using reanalysis data, based on a four weather-type classification (Madonna et al. 2017). For instance, they show that zonal westerly flow (like our weather type 2) is predominantly linked to the central jet position.

Figure 6 shows that each weather type is predominantly associated with a particular sub-region of the space explored by jet latitude and jet strength. For instance, westerlies (WT2) are linked with strong central and northern jets in our PPE, similar to the reanalysis results described above. Conversely, knowing the jet position and strength does not uniquely identify a particular weather type as there is considerable overlap between the sub-regions of jet latitude-strength space for certain weather types. The relationship between jet and weather type is less clear for weather type 1 (northerly); Fig. S2 shows that the pressure patterns that are clustered into weather type 1 can vary a lot conditioned on the position of the jet.

Figures 7 and 8 show that in the second half of the twenty-first century the jet strengthens when in its central and northern locations, and there is a reduction in the amount of time spent in its southern position. Figure 6 shows that the reduction in the frequency of the weather types 1 (Northerly) and 5 (Scandinavian High) and the increase in frequency of westerly weather types (WT2 and WT4) in the future can be explained by a northerly shift and strengthening of the

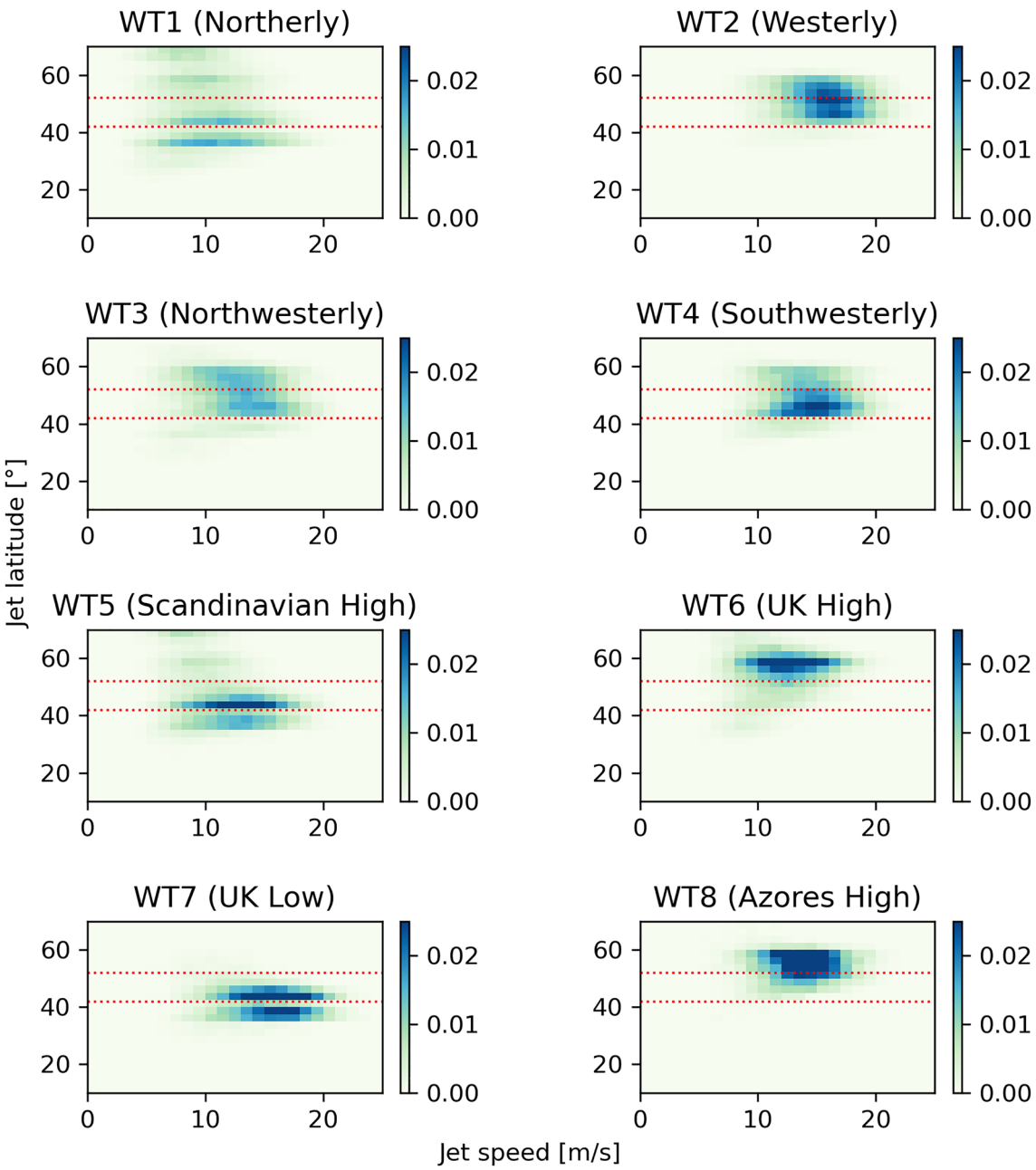


**Fig. 6** The relationship between properties of the eddy-driven jet and the eight weather types in the climate simulations for 1900–2100. Each panel shows the 2-d histogram (values normalised so sum to 1) of daily jet latitude (y-axis) and strength (m/s; x-axis) for winter days when the weather type in the title of the panel occurred. The red dashed lines show the "central" jet position

eddy-driven jet. By comparison with Fig. 6, this northward shift is broadly consistent with the PPE's increase in frequency of weather types 2 and 6 (westerly and UK High) and a decrease in occurrence of weather types 1 and 5 (Northerly and Scandinavian High) seen in Fig. 1 from about 2050 onwards. This timing for fewer days in weather types 1 and 5 is also consistent with the timing of the reduced frequency of the southerly jet (see Fig. 8). However, the central jet steadily becomes more frequent and stronger between 1900 and 2050, after which it remains steady. The northern jet shows a modest reduction in frequency, and then becomes more frequent from 2050 when it also strengthens. Averaged over the PPE, the jet latitude shifts northwards by a degree over the period 2070–2100 (not shown), which is consistent with the amount shown in Barnes and Polvani (2013). Figures 8and S6 show that most members have multidecadal variations in their jet latitude. The PPE contains members that have visible trends towards higher latitudes (like 2491 and 0834,

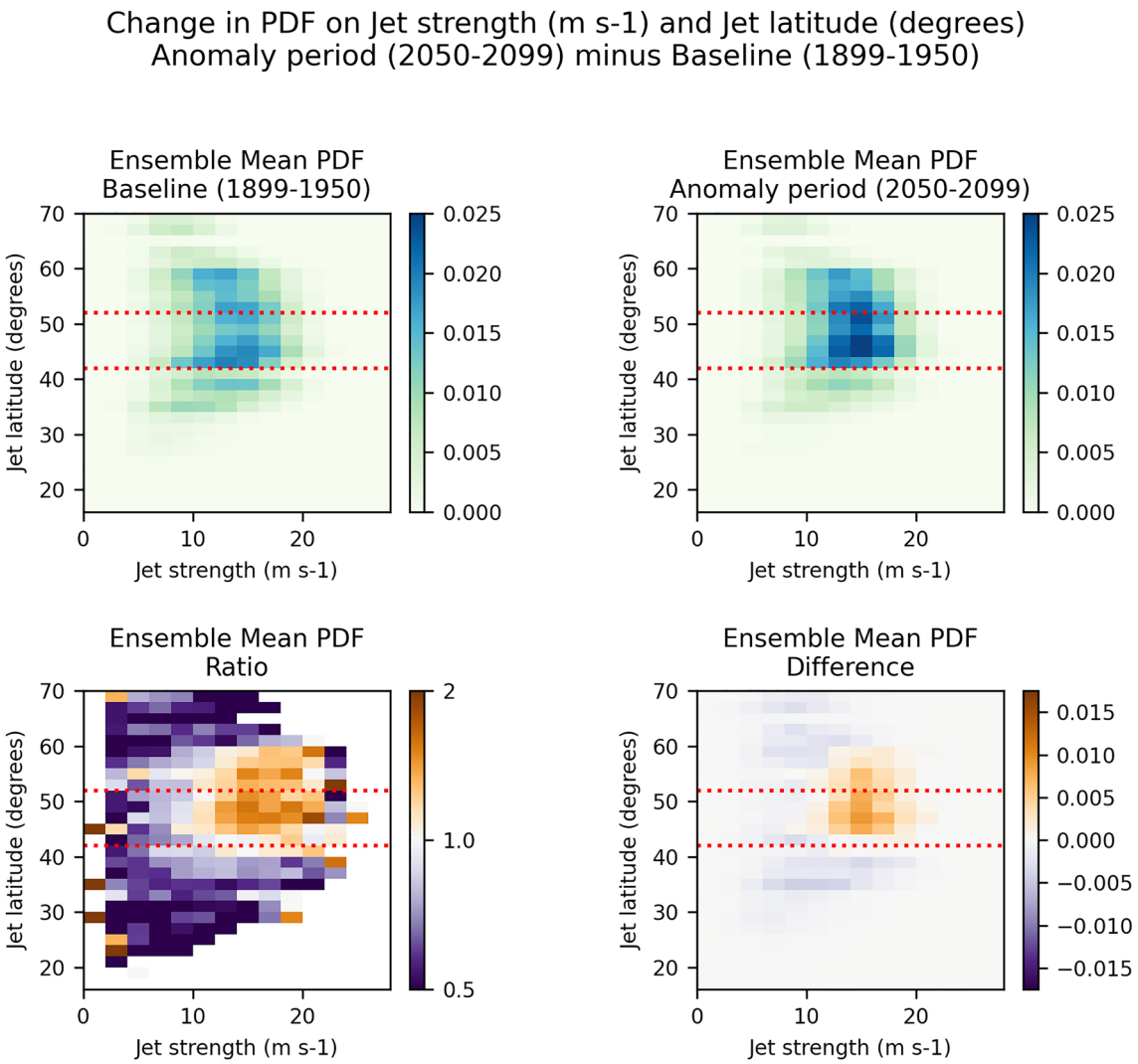


**Fig. 7** Comparison of ensemble mean joint PDF of daily jet latitude and jet strength for winter (DJF) in the baseline period (1900–1949; top left) and future period (2050–2099; top right). Bottom panels show the change in PDF in the future period relative to the baseline period as a ratio (left) and difference (right). PDFs are estimated using the 2-d normalised histogram of daily jet latitude and strength. Red dotted lines denote the "central" jet position

see Fig. S6), some behave similarly to the ensemble mean (like 2868 and 1649) and some retain a relatively southerly jet position throughout the twenty-first century (like 1113 and 0605).

### 5.2 Large-scale drivers of winter variability

Zappa and Shepherd (2017) state that based on the experience of seasonal forecasting, variations in these features of the Atlantic/European circulation arise from three main sources: polar vortex strength, tropical amplification, and polar amplification (see definitions in Sect. 2); we add a fourth, the QBO. We analyse changes in these four drivers to better understand changes in the PPE and compare against CMIP6 to assess robustness of our projections.

Figure 9 shows a diverse set of changes in the strength of the polar vortex with most members lying outside the range of control (unforced) simulations for the last few decades, suggesting these changes are not due to internal variability alone. The members predominantly show a large strengthening in polar vortex strength towards the end of the twenty-first century, with several members at the high end of the CMIP5 range (Manzini et al. 2014). Unfiltered time series of the change in polar vortex strength (see Fig. S7) show that in the top five members of Fig. S6 (2491, 0834, 2123, 1843, and 1649), some of the upward trend is explained by a reduction in winters with a strongly negative (weakened) polar vortex. The tropical amplification (see Fig. 9) shows a strong consistent signal with little diversity across the PPE, consistent with the narrow spread in global warming (see

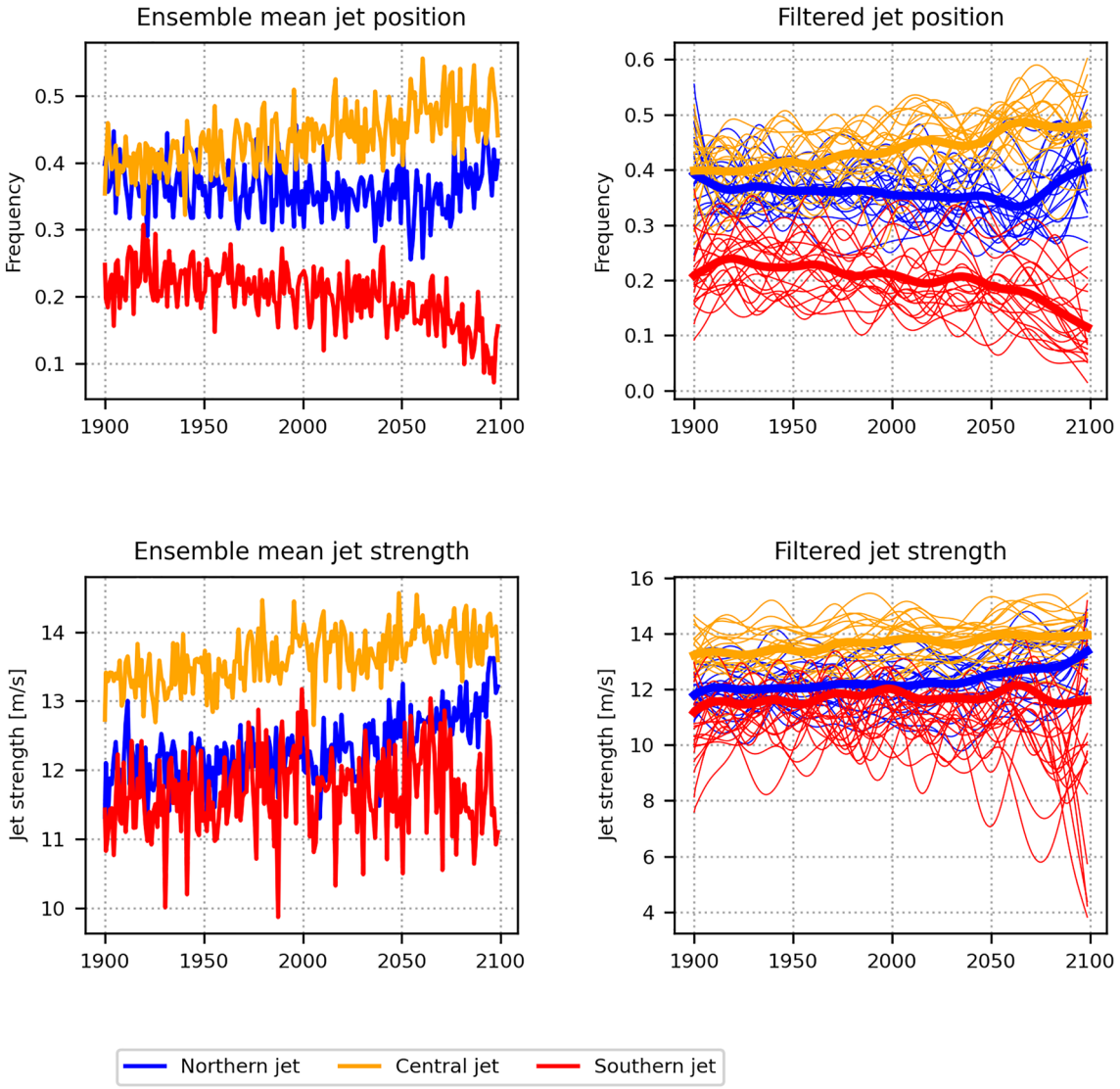


**Fig. 8** Evolution of fraction of winter days spent in each jet latitude band and the jet strength from 1900 to 2100 for the southern, central and northern jet for the ensemble mean (left panels) and as 40-year filtered time series for the ensemble mean and individual PPE members (right panels)

Yamazaki et al. (2021)). The polar amplification behaves similarly, although one PPE member behaves differently due to its drift in the AMOC (see Sect. 2). The QBO shows a clear reduction in the strength of the easterly phase, which implies less drag on the westerly polar vortex (Hall et al. 2015) consistent with a strengthening of the polar vortex.

Analysis over periods of non-stationarity in individual members is problematic because it is easy to misinterpret strong collinearity as seen in Fig. S6 as causal when there is a risk that it might be spurious. However, emergent relationships across PPEs or multimodel ensembles can somewhat alleviate this issue as they explore a range of different trends. Figure 10 shows scatterplots of the changes in weather type frequency against changes in the large-scale drivers between 2050–2099 and 1900–1950. Due to the relatively small sample size, we only show the four relationships where the magnitude of the rank correlation is greater than 0.6. This does not mean that the large-scale drivers are only affecting these four weather types; there are several relationships with correlations between 0.4 and 0.6, which could be causal, but it would require a more detailed analysis to make more robust statements. Large correlations with parameter values across the PPE are indicative of the reason for the diverse spread. Here, a moderate 21% of the spread (not shown) in the polar vortex changes across the PPE is controlled by the Critical Froude number in the Gravity Wave Drag Scheme. We cannot tell whether this is a direct effect of the critical

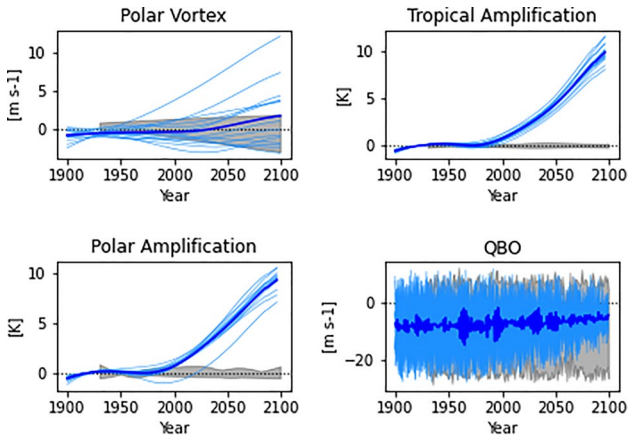


**Fig. 9** Time series of four large-scale drivers of North Atlantic/European circulation for the 15 coupled PPE members (blue), their ensemble mean (dark blue). The grey shading shows the range of changes that correspond to years 1930 to 2100 from control runs forced with 1900 conditions (the first 30 years are excluded due to an initial drift of 0.2K in global temperature in these runs over that period). The QBO is unfiltered but the other three drivers are smoothed with a 40-year filter

Froude number on the response or whether it is indirectly related to changes in the present day state as suggested by (Sigmond and Scinocca 2010).

Into the future, members with a strengthened polar vortex also have a reducing frequency of WT1 and WT5, and an increasing frequency of WT2. These changes are consistent with the known influence of the stratosphere on the North Atlantic surface climate, where a strengthened polar vortex leads to a positive NAO (as discussed in Ineson and Scaife 2009). The change in polar vortex strength also has a sizeable rank correlation of 0.68 with the change in jet strength for the 13 non-drifting AMOC members (0.48 for the 15 members); several possible mechanisms that could provide such a link are discussed in Hall et al. (2015). Consequently, the future changes in pressure patterns, eddy-driven jet, and polar vortex strength are behaving consistently.

Having established the importance of the polar vortex strength in our PPE, and knowing the importance of tropical amplification from Zappa and Shepherd (2017), we compare how the PPE and CMIP6 RCP8.5 projections explore the space defined by these two drivers (see Fig. 11). Unlike Zappa and Shepherd (2017), we do not normalise these by global temperature change. Figure 11 shows that for the end of the twenty-first century (right panel), the PPE extended the range of changes in polar vortex strength sampled by CMIP6 but only explored the top half of the CMIP6 range of tropical amplification. The latter is related to the narrow range of climate feedbacks explored by this PPE (Rostron et al. 2020). For changes up to the early twenty-first century, the space explored by the two ensembles is similar.

## 6 Summary and discussion

We have demonstrated a two-stage approach to explain the range of projected changes across an ensemble of climate simulations. The first stage (based on Figs. 1, 2, 3, 4, 5) aims to describe the range of possible outcomes in a climate hazard, in terms of contributary factors that people can easily relate to. In our case, we have applied this to winter precipitation in regions of the UK, across a 15-member PPE of coupled climate simulations, relating them to a local driver of changes in weather that people are familiar with, namely local pressure patterns. The second stage (based on Figs. 6, 7, 8, 9, 10, 11) involves an analysis to understand the changes in the local driver(s) in terms of larger-scale drivers such as global temperature, temperature gradients, and/or sub-seasonal phenomena that drive year-to-year variability. This deeper understanding is put in the context of results from other climate projections, to assess how representative our projections are with respect to the wider uncertainty, so that users of these climate projections can gauge the extent to which they need to factor in more information.

We find that the projected increase in UK winter precipitation (Fig. 2) predominantly relates to an increase in rainfall intensity across most weather types (Fig. 3), most notably for south-westerlies. The magnitude of intensity change varies across the PPE and is the main source of spread in future UK winter precipitation projections. This increasing intensity also leads to an increase in year-to-year variability of winter precipitation (Fig. 5). However, changes in the frequency of the weather types (Fig. 1) over the twenty-first century also contributes to the projected increase in precipitation and its variability (Figs. 4 and 5). That the UK winter precipitation changes are largely due to an increase in rainfall intensity agrees with Emori and Brown (2005) and Seagar et al. (2010), the latter agreeing that this is largely a thermodynamic effect.

Our breakdown of precipitation by weather type also allows future projections to be better understood in relations to today's weather. For example, if we experienced a period of northerlies and easterlies, we could say that our projections suggest less of these to occur in the future under climate change. Note that quantitative estimates would need to account for the wet biases for England, Wales, and UK as a whole. There are alternatives to our 8 weather types that could have been used. We suggest the choice depends on a trade-off between the level of detail that suits the intended audience, and the level of detail required by the hazard of interest and by the need to provide useful insights. For example, if the four weather types used by Madonna et al. (2017) were expressed in terms of mean sea level pressure rather than geopotential

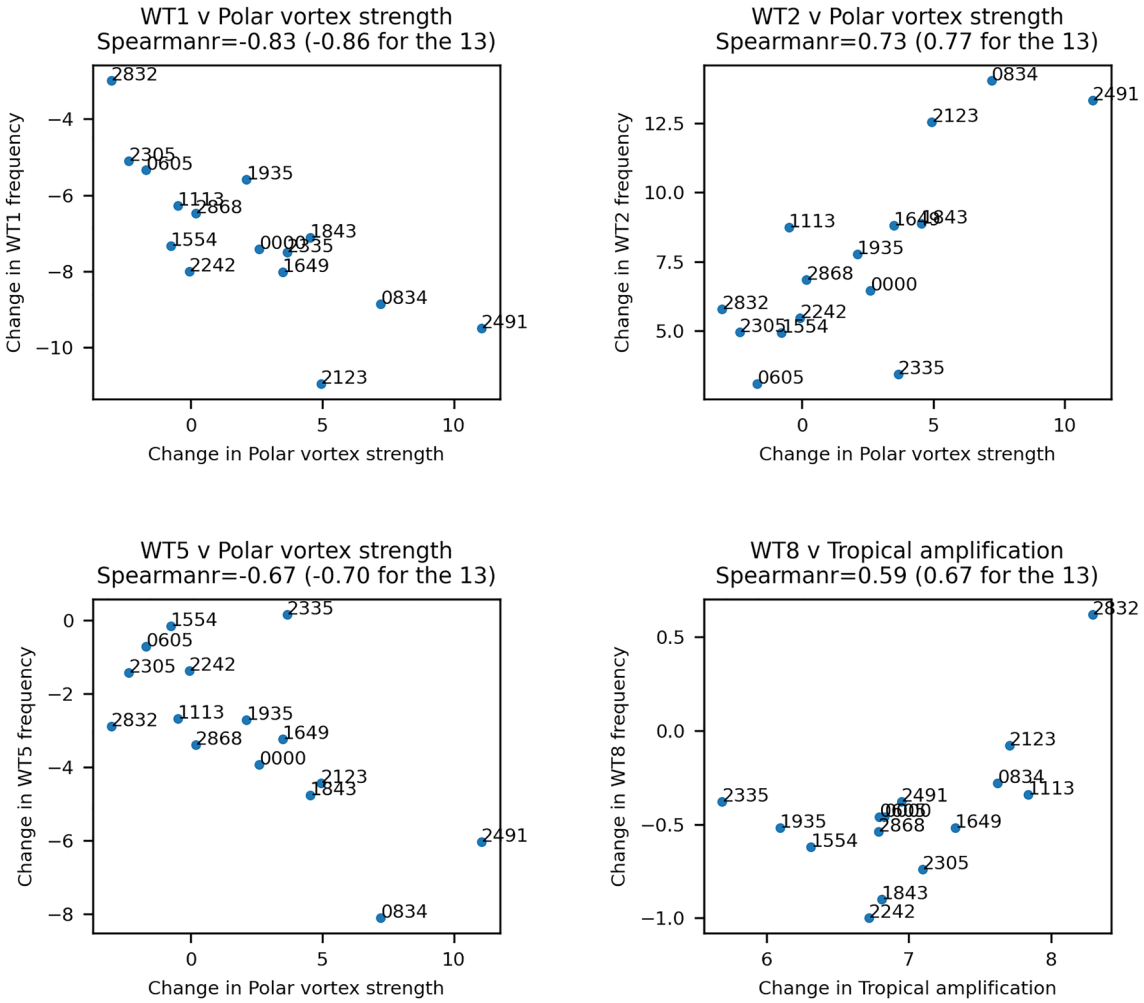


**Fig. 10** Relationships between changes between 2050–2099 and 1900–1950 in the frequency of weather types and the four large-scale drivers across the PPE. Spearman rank correlations in the plot titles are for all 15 members, with a value in brackets for just the 13 members with no AMOC drift. Only relationships where the correlation has a magnitude greater than 0.6 are shown

height, they could have led to slightly simpler messaging; however, it would not have been possible to make the distinction between the greater increase in intensity associated with southwesterlies over westerlies. In contrast, climate extremes might need a more detailed definition of the weather types; Kendon et al. (2020) show an example of how this might work, using the 30 weather types to help explain a different climate variable, the record hottest day in UK winter. A cautionary note from that paper is that the quality of the dependency of the local climate hazard on weather type varies considerably across the multimodel ensemble, suggesting an initial filtering stage is required to omit members with the poorest performance.

Unlike other studies that have had a similar aim to that of our first stage, we have added a second stage where we link the local driver (here it is the weather types) to the larger scale drivers that have been shown to explain most of the variations across climate projections. Across the PPE, the eddy-driven jet strengthens and shifts away from the southern jet position towards the central position and by the late twenty-first century, towards the northern jet (Figs. 7 and 8). The changes in the weather types are consistent with these changes in the eddy-driven jet (Fig. 6). We also analysed four other large-scale drivers (Fig. 9) and found that the changes in the weather types and eddy-driven jet were most strongly linked to changes in the strength of the polar vortex (Fig. 10). Half the PPE members show increases in the strength of the polar vortex. The QBO shows a reduction in the strength of the easterly phase in all members. As the easterly QBO phase favours a weaker polar vortex (Holton and Tan 1982), a reduction in its strength is likely to be contributing a strengthening effect on the polar vortex. This relative importance of the polar vortex strength over the polar and tropical amplification may be because the parameter perturbations (mainly in the gravity wave drag scheme) have been effective in sampling a wide range of changes

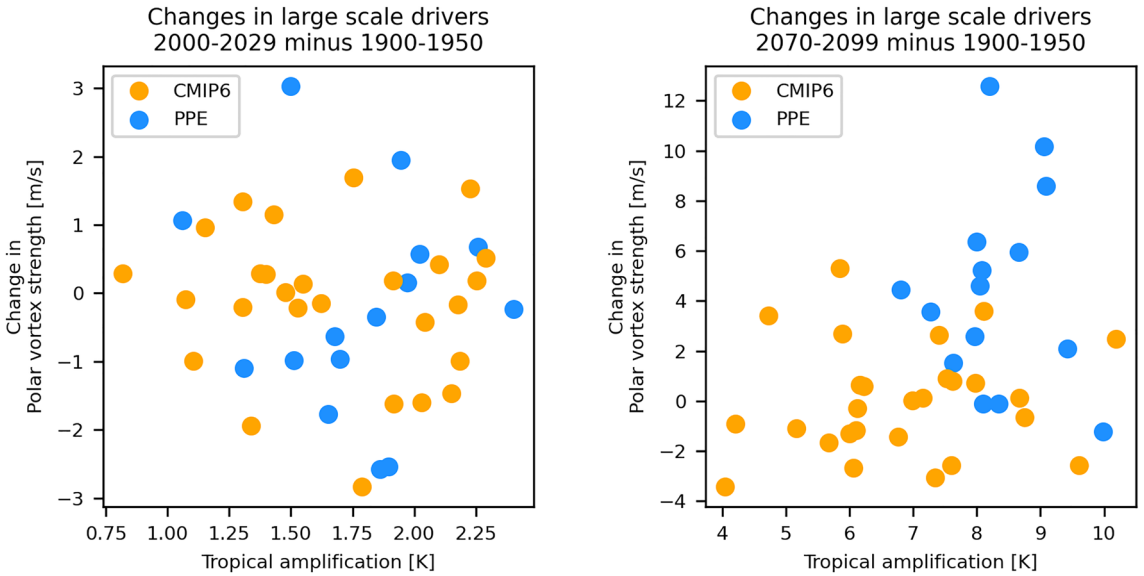


**Fig. 11** Changes in polar vortex strength and tropical amplification from the 1900–1950 baseline, as seen in the PPE and CMIP6 under the RCP8.5 scenario

in the strength of the polar vortex but cover only half the range of the other two key drivers. The lack of spread in tropical warming is largely due to the high-end global warming seen in the PPE, which is mainly because the PPE does not include variants that explore the low end of the climate sensitivity range with plausible model performance (Yamazaki et al. 2021). Figure 11 shows that neither the PPE nor CMIP6 is representative of the full coverage explored by both. We conclude that a combination of both the PPE and CMIP6 provides the best coverage of two key drivers of changes in circulation over the UK.

In practice, studies based on a set of climate simulations are not based on the full set of available climate simulations and therefore not representative of the full range that could be explored by state-of-the-art climate models. There are many reasons for this such as ease of access, availability of the required variables, or that only certain global simulations have been downscaled as in the case of UKCP Regional and UKCP Local. Armed with the information captured in Fig. 11, users can better appreciate how representative their results might be of the range of possibilities. For example, users of the regional simulations from UKCP can see that this ensemble does not represent future climates where the polar vortex weakens and the tropical amplification is at the low end, so that the westerlies become less frequent over the twenty-first century. The assessment also provides useful information if the user wants to sub-sample the PPE members to provide a smaller but representative set of climate simulations to drive impacts studies e.g. (McSweeney and Jones 2016). The analysis from stage one also provides information which could be used for a sub-selection e.g., the members with the least and greatest contribution from changes in weather type frequency, (see Fig. S5).

In general, we have evaluated the robustness of our PPE in terms of changes in key large-scale drivers that dominate variations in the local drivers of stage one across the wider multimodel ensemble. So, a good understanding of the key large-scale drivers is required to inform any assessment of robustness of projections of other variables of interest. This follows the same reasoning behind the choice of the variables used for storylines, which are tailored to the user and are promoted as being better for robust decision-making strategies in the presence of the deep uncertainty that exists in climate adaptation due to imperfect climate models and a limited set of emissions scenarios (Zappa and Shepherd 2017; Dessai et al. 2018; Harvey et al. 2023). So improved causal understanding can benefit both methods. Indeed, in this particular case, the Zappa and Shepherd storyline variables were the ones relevant to our assessment of the robustness.

Improved causal understanding also provides the potential to refine this cloud of values by ruling out PPE or CMIP6 members that are relatively poor in representing key processes involving the large-scale drivers. However, any future research on this will be challenging as there are often multiple causal factors to consider (e.g., Hall et al. 2015; Kretschmer et al. 2016; Andrews et al. 2019). Indeed, there are already signs of one such causal driver occurring in some of the PPE members; the driver is sea ice melt in the Barents and Kara seas which leads to an additional weakening of the polar vortex (Manzini et al. 2018; Kretschmer et al. 2020). In Fig. 9 there is a decrease

in the polar vortex strength during the early twenty-first century at the same time that the sea ice melts; this will be more carefully investigated in future work.

The assessment of robustness of a new ensemble requires comparison with a larger set of simulations that could include the CMIP5 and CMIP6 multimodel ensembles, the so-called SMILEs (single model initial condition large ensembles), and realisations from very high resolution global and regional climate models. Even with a large, combined set of climate simulations from several of these sources, there are still sampling issues, and more importantly systematic errors, that limit how well the full range of possible future outcomes for the climate hazard are represented. For instance, studies that identify systematic errors common to all current models, such as Screen et al. (2022) who suggest the current models generally under-predict equatorward movement of the jet in response to Arctic sea ice melt, imply that there are possible future climates outside the range as it is currently explored. New methods are needed to estimate the wider uncertainty accounting for such issues; but it will still be essential to evaluate the climate projections in this context.

**Supplementary Information** The online version contains supplementary material available at https://doi.org/10.1007/s00382-024-07165-7.

**Acknowledgements** This work was supported by the Met Office Hadley Centre Climate Programme funded by DSIT. Thanks also to David Fereday for the original weather typing code, to Ted Shepherd for useful advice on the stratospheric polar vortex, and James Pope for sharing of useful information on the weather types. We acknowledge the World Climate Research Programme, which, through its Working Group on Coupled Modelling, coordinated and promoted CMIP6. We thank the climate modelling groups for producing and making available their model output, the Earth System Grid Federation (ESGF) for archiving the data and providing access, and the multiple funding agencies who support CMIP6 and ESGF.

**Author contributions** David, Carol and Fai contributed to the concept of the paper. David, Carol, and Kuniko were involved in the design of the coupled simulations, which were run by Kuniko. Hazel processed the weather types, Philip the jet diagnostics. David did all the analysis and wrote the manuscript. All authors commented on the submitted draft of the paper, notably Hazel, Philip, and Carol.

**Funding** This work was supported by the Met Office Hadley Centre Climate Programme funded by Department for Science, Innovation, and Technology (GB).

**Data availability** The data is available at Zenodo under Doi https://doi.org/10.5281/zenodo.10043509. The code used to make the figures can be found at https://github.com/qump-project/qump-hadgem3/tree/master/code/papers/UKWinterPrecip2023 under a Crown Copyright BSD3 license.

## Declarations

**Conflict of interest** The authors have no relevant financial or non-financial interests to disclose.



## References

Andrews MB, Knight JR, Scaife AA et al (2019) Observed and simulated teleconnections between the stratospheric Quasi-Biennial oscillation and northern hemisphere winter atmospheric circulation. J Geophys Res Atmos. https://doi.org/10.1029/2018JD029368

Arnell NW, Kay AL, Freeman A et al (2020) Changing climate risk in the UK: a multi-sectoral analysis using policy-relevant indicators. Clim Risk Manag. https://doi.org/10.1016/j.crm.2020.100265

Barnes EA, Polvani L (2013) Response of the midlatitude jets, and of their variability, to increased greenhouse gases in the CMIP5 models. J Clim 26:7117–7135. https://doi.org/10.1175/JCLI-D-12-00536.1

Baumberger C, Knutti R, Hirsch Hadorn G (2017) Building confidence in climate model projections: an analysis of inferences from fit. Wiley Interdiscip Rev Clim Chang 8:e454

BBC (2020) Sport 2050: climatecast - a weather forecast from the future. https://www.bbc.co.uk/sport/56972367

Bony S, Dufresne JL, Le Treut H et al (2004) On dynamic and thermodynamic components of cloud changes. Clim Dyn 22:71–86. https://doi.org/10.1007/s00382-003-0369-6

Caldwell PM, Zelinka MD, Klein SA (2018) Evaluating emergent constraints on equilibrium climate sensitivity. J Clim 31:3921–3942. https://doi.org/10.1175/JCLI-D-17-0631.1

Collins M, Booth BBB, Bhaskaran B et al (2011) Climate model errors, feedbacks and forcings: a comparison of perturbed physics and multi-model ensembles. Clim Dyn 36:1737–1766. https://doi.org/10.1007/s00382-010-0808-0

Davies PA, McCarthy M, Christidis N et al (2021) The wet and stormy UK winter of 2019/2020. Weather. https://doi.org/10.1002/wea.3955

Dessai S, Bhave A, Birch C et al (2018) Building narratives to characterise uncertainty in regional climate change through expert elicitation. Environ Res Lett. https://doi.org/10.1088/1748-9326/aabcdd

Dunstone N, Smith D, Scaife A et al (2016) Skilful predictions of the winter North Atlantic oscillation one year ahead. Nat Geosci 9:809. https://doi.org/10.1038/ngeo2824

Emori S, Brown SJ (2005) Dynamic and thermodynamic changes in mean and extreme precipitation under changed climate. Geophys Res Lett. https://doi.org/10.1029/2005GL023272

Eyring V, Bony S, Meehl GA et al (2016) Overview of the coupled model intercomparison project phase 6 (CMIP6) experimental design and organization. Geosci Model Dev. https://doi.org/10.5194/gmd-9-1937-2016

Fabiano F, Christensen HM, Strommen K et al (2020) Euro-Atlantic weather regimes in the PRIMAVERA coupled climate simulations: impact of resolution and mean state biases on model

performance. Clim Dyn 54:5031–5048. https://doi.org/10.1007/s00382-020-05271-w
Fabiano F, Meccia VL, Davini P et al (2021) A regime view of future atmospheric circulation changes in northern mid-latitudes. Weather Clim Dyn 2:163–180. https://doi.org/10.5194/wcd-2-163-2021
Fereday DR, Knight JR, Scaife AA et al (2008) Cluster analysis of North Atlantic-European circulation types and links with tropical Pacific sea surface temperatures. J Clim 21:3687–3703. https://doi.org/10.1175/2007JCLI1875.1
Fosser G, Kendon E, Chan S et al (2020) Optimal configuration and resolution for the first convection-permitting ensemble of climate projections over the United Kingdom. Int J Climatol 40:3585–3606. https://doi.org/10.1002/joc.6415
Garry FK, Bernie DJ (2023) Characterizing temperature and precipitation multi-variate biases in 12 and 2.2 km UK climate projections. Int J Climatol. https://doi.org/10.1002/joc.8006
Hall R, Erdelyi R, Hanna E et al (2015) Drivers of North Atlantic polar front jet stream variability. Int J Climatol 35:1697–1720. https://doi.org/10.1002/joc.4121
Hanlon HM, Bernie D, Carigi G, Lowe JA (2021) Future changes to high impact weather in the UK. Clim Chang. https://doi.org/10.1007/s10584-021-03100-5
Harvey B, Hawkins E, Sutton R (2023) Storylines for future changes of the North Atlantic jet and associated impacts on the UK. Int J Climatol 43:4424–4441. https://doi.org/10.1002/joc.8095
Haylock MR, Hofstra N, Klein Tank AMG et al (2008) A European daily high-resolution gridded data set of surface temperature and precipitation for 1950–2006. J Geophys Res Atmos. https://doi.org/10.1029/2008JD010201
Holton JR, Tan H-C (1982) The Quasi-Biennial oscillation in the Northern Hemisphere lower stratosphere. J Meteorol Soc Jpn Ser II 60:140–148. https://doi.org/10.2151/jmsj1965.60.1_140
Huntingford C, Marsh T, Scaife AA et al (2014) Potential influences on the United Kingdom's floods of winter 2013/14. Nat Clim Chang 4:769–777. https://doi.org/10.1038/NCLIMATE2314
Ineson S, Scaife AA (2009) The role of the stratosphere in the European climate response to El Nino. Nat Geosci 2:32–36. https://doi.org/10.1038/NGEO381
Jones RN, Patwardhan A, Cohen SJ, et al (2015) Foundations for decision making. In: Climate change 2014 impacts, adaptation and vulnerability: part a: global and sectoral aspects
Kay JE, Deser C, Phillips A et al (2015) The community earth system model (CESM) large ensemble project: a community resource for studying climate change in the presence of internal climate variability. Bull Am Meteorol Soc. https://doi.org/10.1175/BAMS-D-13-00255.1
Kendon M, Sexton D, McCarthy M (2020) A temperature of 20°C in the UK winter: a sign of the future? Weather 75:318–324. https://doi.org/10.1002/wea.3811
Kendon E, Short C, Pope J et al (2021) Update to UKCP local (2.2km) projections. Met Office, July 2021. https://www.metoffice.gov.uk/pub/data/weather/uk/ukcp18/science-reports/ukcp18_local_update_report_2021.pdf
Kennedy-Asser AT, Andrews O, Mitchell DM, Warren RF (2021) Evaluating heat extremes in the UK climate projections (UKCP18). Environ Res Lett. https://doi.org/10.1088/1748-9326/abc4ad
Kretschmer M, Coumou D, Donges JF, Runge J (2016) Using causal effect networks to analyze different arctic drivers of mid-latitude winter circulation. J Clim. https://doi.org/10.1175/JCLI-D-15-0654.1
Kretschmer M, Zappa G, Shepherd TG (2020) The role of Barents-Kara sea ice loss in projected polar vortex changes. Weather Clim Dyn 1:715–730. https://doi.org/10.5194/wcd-1-715-2020
Madonna E, Li C, Grams CM, Woollings T (2017) The link between eddy-driven jet variability and weather regimes in the North Atlantic-European sector. Q J R Meteorol Soc. https://doi.org/10.1002/qj.3155
Maidens A, Knight JR, Scaife AA (2021) Tropical and stratospheric influences on winter atmospheric circulation patterns in the North Atlantic sector. Environ Res Lett 16:24035. https://doi.org/10.1088/1748-9326/abd8aa
Manzini E, Karpechko AY, Anstey J et al (2014) Northern winter climate change: assessment of uncertainty in CMIP5 projections related to stratosphere-troposphere coupling. J Geophys Res. https://doi.org/10.1002/2013JD021403
Manzini E, Karpechko AY, Kornblueh L (2018) Nonlinear response of the Stratosphere and the North Atlantic-European climate to global warming. Geophys Res Lett 45:4255–4263. https://doi.org/10.1029/2018GL077826
McSweeney CF, Jones RG (2016) How representative is the spread of climate projections from the 5 CMIP5 GCMs used in ISI-MIP? Clim Serv 1:24–29. https://doi.org/10.1016/j.cliser.2016.02.001
Met Office Hadley Centre (2020) UKCP global (60km) - European circulation indices. Centre for Environmental Data Analysis. https://catalogue.ceda.ac.uk/uuid/6e61f79cb6b0457eb84edaffcf0aab3a. Accessed 1 June 2020
Moreno-Chamarro E, Caron LP, Ortega P et al (2021) Can we trust CMIP5/6 future projections of European winter precipitation? Environ Res Lett. https://doi.org/10.1088/1748-9326/abf28a
Murphy JM, Harris GR, Sexton DMH et al (2018) UKCP18 Land Projections. Sci Rep 2018:1–191
Neal R, Fereday D, Crocker R, Comer RE (2016) A flexible approach to defining weather patterns and their application in weather forecasting over Europe. Meteorol Appl. https://doi.org/10.1002/met.1563
Pidgeon N, Fischhoff B (2011) The role of social and decision sciences in communicating uncertain climate risks. Nat Clim Chang 1:35–41
Pope JO, Brown K, Fung F et al (2021) Investigation of future climate change over the British Isles using weather patterns. Clim Dyn. https://doi.org/10.1007/s00382-021-06031-0
Rostron JW, Sexton DMH, McSweeney CF et al (2020) The impact of performance filtering on climate feedbacks in a perturbed parameter ensemble. Clim Dyn. https://doi.org/10.1007/s00382-020-05281-8
Scaife AA, Arribas A, Blockley E et al (2014a) Skillful long-range prediction of European and North American winters. Geophys Res Lett 41:2514–2519. https://doi.org/10.1002/2014GL059637
Scaife AA, Athanassiadou M, Andrews M et al (2014b) Predictability of the quasi-biennial oscillation and its northern winter teleconnection on seasonal to decadal timescales. Geophys Res Lett 41:1752–1758. https://doi.org/10.1002/2013GL059160
Screen JA, Eade R, Smith DM et al (2022) Net equatorward shift of the jet streams when the contribution from sea-ice loss is constrained by observed eddy feedback. Geophys Res Lett. https://doi.org/10.1029/2022GL100523
Seager R, Naik N, Vecchi GA (2010) Thermodynamic and dynamic mechanisms for large-scale changes in the hydrological cycle in response to global warming. J Clim. https://doi.org/10.1175/2010JCLI3655.1
Sexton DMH, McSweeney CF, Rostron JW et al (2021) A perturbed parameter ensemble of HadGEM3-GC3.05 coupled model projections: part 1: selecting the parameter combinations. Clim Dyn 56:3395–3436. https://doi.org/10.1007/s00382-021-05709-9
Sigmond M, Scinocca JF (2010) The influence of the basic state on the Northern Hemisphere circulation response to climate change. J Clim 23:1434–1446. https://doi.org/10.1175/2009JCLI3167.1
Williams KD, Webb MJ (2009) A quantitative performance assessment of cloud regimes in climate models. Clim Dyn 33:141–157. https://doi.org/10.1007/s00382-008-0443-1

Williams KD, Copsey D, Blockley EW et al (2018) The met office global coupled model 3.0 and 3.1 (GC3.0 and GC3.1) configurations. J Adv Model Earth Syst. https://doi.org/10.1002/2017MS001115

Woollings T, Hannachi A, Hoskins B (2010) Variability of the North Atlantic eddy-driven jet stream. Q J R Meteorol Soc. https://doi.org/10.1002/qj.625

Yamazaki K, Sexton DMH, Rostron JW et al (2021) A perturbed parameter ensemble of HadGEM3-GC3.05 coupled model projections: part 2: global performance and future changes. Clim Dyn 56:3437–3471. https://doi.org/10.1007/s00382-020-05608-5

Zappa G, Shepherd TG (2017) Storylines of atmospheric circulation change for European regional climate impact assessment. J Clim 30:6561–6577. https://doi.org/10.1175/JCLI-D-16-0807.1

Zhang W, Furtado K, Wu P et al (2021) Increasing precipitation variability on daily-to-multiyear time scales in a warmer world. Sci Adv. https://doi.org/10.1126/sciadv.abf8021